




Research Article

# Sealing of glass with titanium by glass pressing at the softening point

Sebastian Winkler<sup>1</sup> · Jan Edelmann<sup>1</sup>  · Daniel Günther<sup>1</sup> · Sebastian Wieland<sup>1</sup> · Franz Selbmann<sup>2</sup> · Mario Baum<sup>2</sup> · Andreas Schubert<sup>1,3</sup>

© Springer Nature Switzerland AG 2019

## Abstract

Hermetic and mechanically strong glass-to-metal seals are required for many applications in technological fields such as aerospace engineering or medical engineering. While traditional glass-to-metal bonding technologies require melting of the glass, modern technologies such as anodic bonding use glass in its solid state. In this publication, a novel glass-to-metal bonding method with process temperatures around the softening point of the glass material is investigated. A glass window (silica based crown glass B270) in a titanium (grade 5) housing is manufactured by applying compressive force to the glass in a controlled low pressure argon atmosphere. Adherence of the glass-to-metal interface is determined with a universal testing machine. Hermeticity is measured directly with either pressure gain test or helium leak test. Experiments were performed in a full factorial design with 3 different process temperatures, 3 different process forces and 3 different methods for preparing the titanium surface. The results indicate that the bonding method is capable of producing hermetic seals with leak rates below  $10^{-8}$  mbar l/s. Roughening of the metal surface generally improves both hermeticity and interface strength. Bonding strength can be further improved by increasing either processes temperature or, especially for rough surfaces, process force. For improving hermeticity either processes temperature or, especially for smooth surfaces, process force must be increased. The results indicate that successful bonding of glass and titanium with the new bonding method is influenced by the effects of mechanical interlocking and chemical reactions at the material interface.

**Keywords** Glass · Glass-to-metal seals · Titanium · Hermetic seal

## List of symbols

$T_p$  Process temperature (glass pressing)  
 $F_p$  Process force (glass pressing)  
 $Q_L$  Leak rate  
 $F_F$  Failure force  
 $Ra$  Mean roughness

require melting of the glass, modern technologies such as anodic bonding use glass in its solid state. The specific investigations are motivated by an application in medical engineering, where an implantable electronic device is encapsulated in a hermetic titanium housing with an optical window for infrared data communication, for which patent protection has been sought [5]. This is the preferred encapsulation strategy for a myoelectric hand prosthesis control that Winkler et al. [23] investigated for the encapsulation of implantable electronics. The influence of the manufacturing parameters on the bond strength and the hermeticity of the seal is the object of the investigations.

In this paper a new approach for bonding glass to titanium is evaluated experimentally. A glass window in a

## 1 Introduction: need and proposal

Hermetic and mechanically strong glass-to-metal seals are required for many applications in technological fields such as aerospace engineering or medical engineering. While traditional glass-to-metal bonding technologies

✉ Jan Edelmann, jan.edelmann@iwu.fraunhofer.de | <sup>1</sup>Institute for Machine Tools and Forming Technology, Fraunhofer IWU, Chemnitz, Germany. <sup>2</sup>Institute for Electronic Nano Systems, Fraunhofer ENAS, Chemnitz, Germany. <sup>3</sup>Professorship Micromanufacturing Technology, TU Chemnitz, Chemnitz, Germany.



SN Applied Sciences (2019) 1:562 | <https://doi.org/10.1007/s42452-019-0574-5>

Received: 11 March 2019 / Accepted: 6 May 2019 / Published online: 14 May 2019

titanium housing is manufactured by glass pressing, a technology originally used for manufacturing optical components by glass forming at temperatures slightly below the softening point. With the new approach the problems with high process temperatures and chemical reactions of the bonding methods based on glass melting can be avoided. At the same time, the approach overcomes the limitations of low-temperature bonding methods such as anodic bonding.

## 2 Analysis of existing work

Bonding glasses to metals for decorative coatings can be traced back to ancient Egyptian times. The industrial production of enamelled cookingware and other protective glass coatings on metal surfaces was established in the nineteenth century, followed by many other applications such as the light bulb. Modern applications can be found in biomedical and aerospace engineering, where especially bonding of titanium to glass is of major significance. A good overview of biomedical applications can be found in Gomez-Vega et al. [9] and in the book by Donald [3] on glass-to-metal seals in general.

Traditionally, glass-to-metal seals and glass coatings are produced by melting the glass, allowing it to wet the metal surface and form an interface. Most applications and products with glass-to-metal interfaces such as electrical feedthroughs or protective glass coatings as described in Donald [2] and Donald et al. [4] can be bonded with glass melting technologies. However, the required process temperatures (typical 800 ... 1200 °C) for glass melting limit the number of metals and alloys that can be bonded with glass. In addition, lots of glass metal combinations tend to unfavourable chemical reactions at high temperatures which weaken the interface. Bonding of glass to titanium and its alloys at high temperatures have been studied extensively. Surveys works and meanwhile standard are the works of King et al. [11], Passerone et al. [19] and Goldstein et al. [6]. Kitsugi et al. [12] and Pazo et al. [20] focus on implant applications. Gomez-Vega et al. [8] and Peddi et al. [21] deal with the combination of bioactive glasses with titanium.

Throughout the past decades many alternative glass-to-metal bonding technologies with low process temperatures have been reported. Anodic bonding uses static electric fields and mild pressure to produce high quality glass-to-metal seals at temperatures of 200 ... 450 °C. Briand et al. [1] give an overview on anodic bonding, Wei et al. [22] and

Li et al. [16] concentrate on low temperature anodic bonding and especially the sealing of titanium wafers with glass for microfluidic applications is described by Khandan et al. [10]. However, very low surface roughness and flat glass and metal substrates are required for anodic bonding, thus limiting the applications by geometric constraints. Kuckert et al. [13] describes another bonding technology based on ultrasonic welding and demonstrates that glasses and metals can be bonded without melting the glass.

## 3 Experimental procedure

### 3.1 Sample preparation

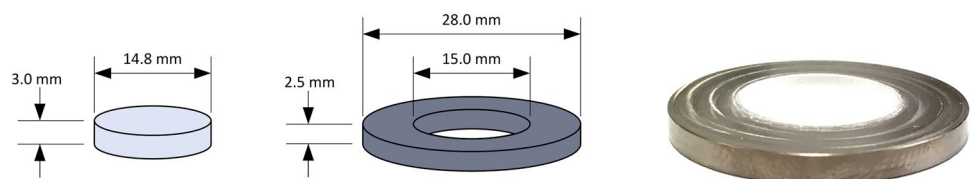
A window-type geometry with a glass sample in the centre of a surrounding titanium ring was used for experiments. Sample dimensions are illustrated in Fig. 1. The titanium alloy Ti6Al4V (Grade 5) was selected because it has an industrial share of more than 50% and it is one of the most relevant alloys in medical engineering, as Luetjering and Williams [18] discuss in their book about titanium. Samples were machined from Ti6Al4V sheet material by milling. The glass type B270 (by Schott) used for experiments is a silica based optical crown glass and was selected because its thermal expansion coefficient ( $10.3 \times 10^{-6} \text{ K}^{-1}$  for 20 ... 500 °C) matches closely to Ti6Al4V ( $9.5 \times 10^{-6} \text{ K}^{-1}$  for 20 ... 500 °C) as well as its availability and use in technology. The glass material composition is summarised in Table 1. Glass samples were prepared from plate material by water jet machining.

All titanium rings were manufactured by milling. In the next step for some samples the inside surface to be bonded with the glass was roughened by blasting with glass beads (type 09-0011 by Baltrusch & Mütsch, particle size 75... 150 µm) and sharpe edged glass powder (type 09-0010 by Baltrusch & Mütsch) in a micro blasting tool (model HPS by Texas Airsonic). Tactile roughness measurement (Hommel-ETAMIC TurboWave V7.55) was applied to all 3 metal surface types, resulting in values of

**Table 1** Material composition of B270 glass type (mass% of oxides)

SiO <sub>2</sub>	B <sub>2</sub> O <sub>3</sub>	Na <sub>2</sub> O	K <sub>2</sub> O	BaO	Al <sub>2</sub> O <sub>3</sub>
69.1	10.8	10.4	6.2	3.1	0.4

**Fig. 1** Dimensions of glass (left) and titanium (middle) samples. Sample after bonding (right)



$Ra = 0.34 \mu\text{m}$  (milled),  $Ra = 1.15 \mu\text{m}$  (glass bead blasted) and  $Ra = 1.71 \mu\text{m}$  (glass powder blasted). In addition, metal surfaces were analysed with scanning electron microscopy (SEM) and energy-dispersive X-ray spectroscopy (EDS) (model 1450VP by LEO).

### 3.2 Bonding method

In Fig. 4 the bonding process (a) based on glass pressing is illustrated together with the subsequent measurement procedures. After ultrasonic cleaning in ethanol for 5 min the samples are heated to the process temperature  $T_p$  in a controlled atmosphere of argon at a pressure of 5 mbar. By applying compressive force (process force  $F_p$ ) with a die the glass is formed and bonded to the metal surface in the spacing of the titanium ring. A customized glass pressing tool (Fig. 2) based on a universal testing machine is used for the bonding process. Both sample holder and die are located in a vacuum chamber and can be heated up to  $1000^\circ\text{C}$ .

The heaters are equipped with four type K thermocouples for both temperature measurement and temperature control. For the calibration of the temperature measurement a glass-titanium-sample has been prepared with two extra thermocouples, allowing for a direct measurement of the temperatures close to the glass-titanium-interface. Considering the precision of the thermocouples and the calibration method, a total error of  $\Delta T = \pm 5\text{K}$  must be assumed.

In Fig. 3 the different process steps of the glass pressing process can be observed. After heating contact is made between die and glass (A), followed by a 30 s time period (B) allowing the glass to reach its final temperature. The force is raised using a constant rate within 5 s (C), remains constant at the value of what is defined as the process

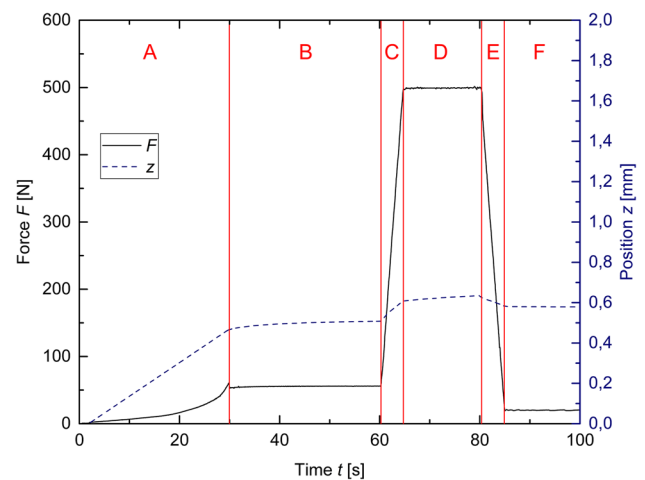


**Fig. 3** Different process steps during glass pressing process (see text for details)

force  $F_p$  for 15 s (D) and decreases for another 5 s (E), followed by the cooldown step (F). The process times for (C), (D) and (E) were fixed for all experiments in order to study the processes at the glass-to-metal interface with comparable conditions.

### 3.3 Adherence

For determination of adherence direct methods and indirect methods are available. Different direct pull-off adhesion tests can be compared in Peddi et al. [21] for borate glass coatings, Wei et al. [22] for anodic bonded wafers and Goller [7] for plasma sprayed bioglass on titanium. In contrast, Lopez-Esteban et al. [17] used the indirect method of Vickers indentation to characterize bioactive glass coatings.

**Fig. 2** Glass pressing tool, based on a universal testing machine with vacuum chamber and heating system

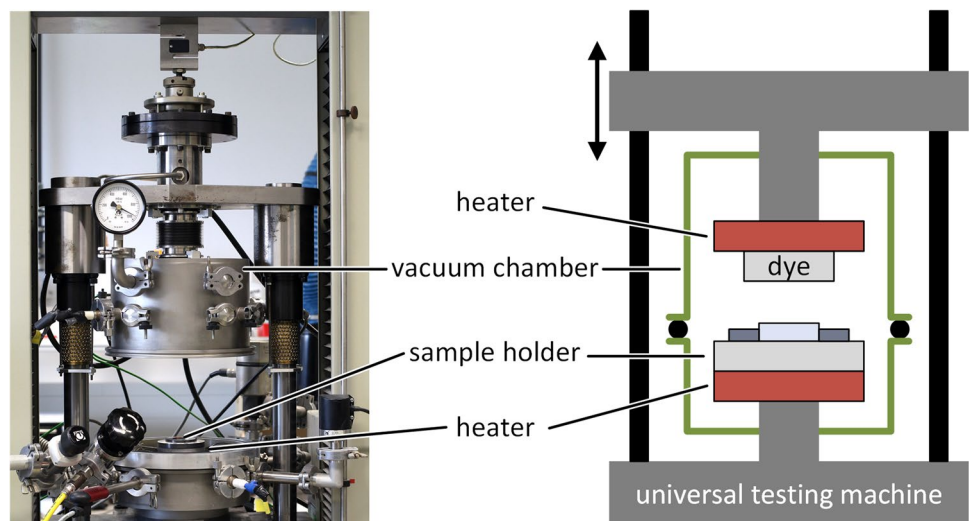
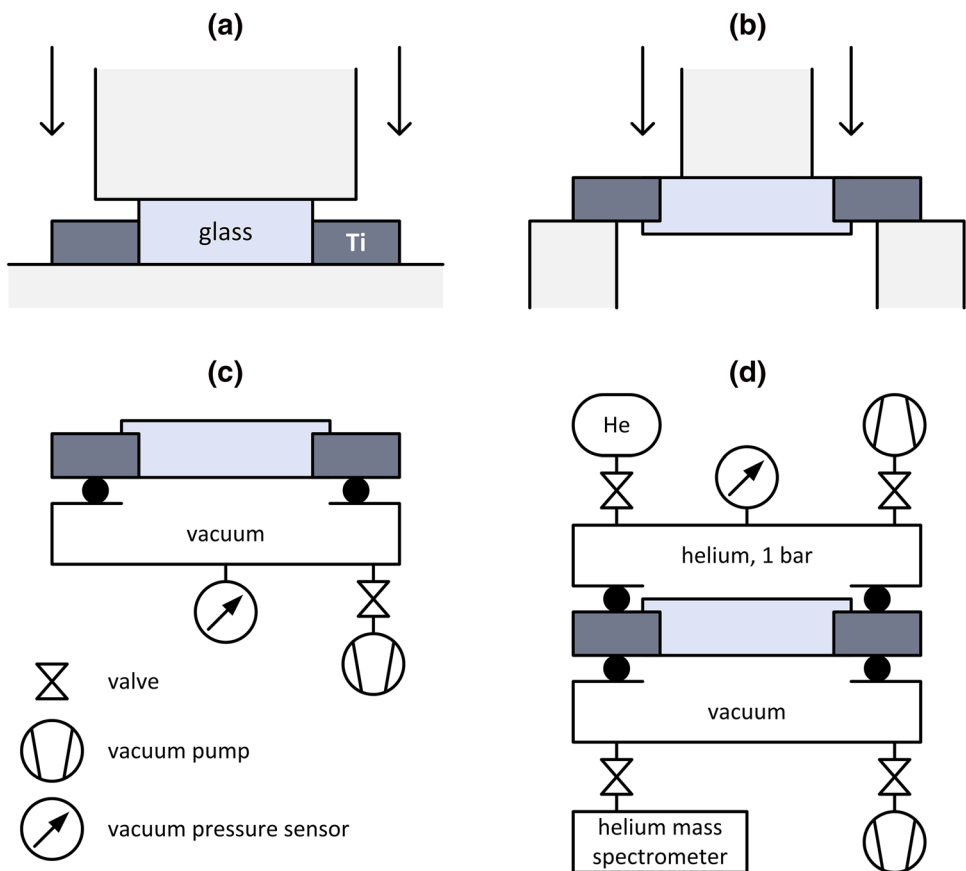


**Fig. 4** Structural principles of experimental procedures; **a** glass pressing glass-to-metal bonding process; **b** determination of adherence by applying force to the glass window; **c** measurement of hermeticity with pressure gain test; **d** measurement of hermeticity with helium leak test; see text for further details



In this investigation a direct method as illustrated in Fig. 4b is applied. A die (diameter 14 mm) is centered on the glass. Compressive force is applied to the die with a universal testing machine at a constant rate of 20 N/s between 0 and 1000 N and 200 N/s for more than 1000 N. The maximum force is recorded as the failure force  $F_3$  for further analysis.

### 3.4 Seal hermeticity

For experimental determination of hermeticity a number of test methods are available. The helium leak test as applied by Lei et al. [15] and technically described by Kutzke [14] is an accredited method and provides accurate results down to leak rates of  $10^{-9}$  mbar l/s. However, for samples with low hermeticity the pressure difference of 1 bar can cause interface failure during helium leak test which leads to damage of the helium leak detector. Therefore, the pressure gain test was used as a second test method. All samples were measured by pressure gain test first and only samples with leak rate values better than  $Q_L < 10^{-4}$  mbar l/s were measured again by helium leak test.

The pressure gain test is specified as procedure D2 in EN 1779 and illustrated in Fig. 4c. One side of the sample

is sealed to a vacuum chamber, which is then evacuated with a vacuum pump. After reaching the base pressure, the valve to the pump is closed and the pressure is recorded over time. The leak rate  $Q_L$  is calculated with the effective chamber volume  $V$  and the linear pressure gain  $dp/dt$  according to Eq. 1. With the system used in this investigation a leak rate up to approx.  $10^{-5}$  mbar l/s can be measured with the pressure gain test.

$$Q_L = V \cdot \left( \frac{dp}{dt} \right) \tag{1}$$

The helium leak test is specified as procedure A1 in EN 1779 and illustrated in Fig. 4d. After evacuation of both vacuum chambers the top chamber is filled with helium to a pressure of 1 bar, a state described as helium standard conditions. The helium flow through the sample is measured with a mass spectrometer as part of a helium leak detector (model QualyTest by Pfeiffer Vacuum), which directly displays the resulting helium leak rate.

### 3.5 Process parameters

A full factorial design of experiments with 3 parameters (machining state of titanium surface, process temperature

$T_p$  process force  $F_p$ ) and 3 values per parameter was chosen for the investigation (see Table 2 in chapter 3). For each parameter combination 2 individual samples were prepared, resulting in 54 samples in total.

Figure 5 shows the viscosity of B270 as a function of temperature. The 3 operating points (705 °C, 745 °C and 785 °C) selected for experiments cover a range of roughly 1.5 orders of magnitude in viscosity and are located close to the softening point. The parameter range was restricted towards higher viscosities because glass pressing with a fixed process time of 15 s would not allow for contact of glass with the metal.

With a sample diameter of 15 mm the selected process force values (200 N, 500 N and 1200 N) correspond to compressive stress in the range of 1 MPa to 7 MPa, which are typical in glass pressing for manufacturing of optical components. Much higher values cannot be used because this may lead to damage of the dies.

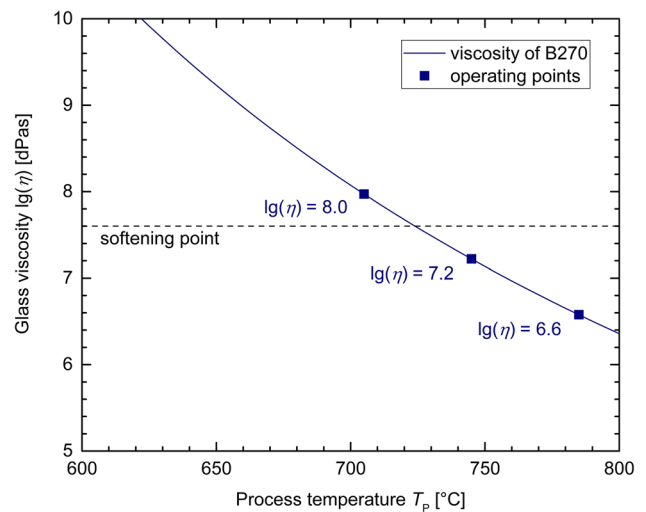


Fig. 5 Viscosity of glass type B270 and working points

**Table 2** Results of leak rate and failure force for different process parameters

Surface	$T_p$ (°C)	$F_p$ (N)	$Q_L$ (mbar l/s)	$F_F$ (kN)
S1 (milled)	705	200	2.3E-02 <sup>a</sup>	0.31
		500	1.1E-01 <sup>a</sup>	1.06
		1200	3.2E-01 <sup>a</sup>	1.59
	745	200	1.2E-01 <sup>a</sup>	0.79
		500	1.1E-01 <sup>a</sup>	2.41
		1200	2.6E-06	3.65
	785	200	1.2E-06	9.02
		500	1.5E-06	11.46
		1200	3.9E-09	10.19
S2 (glass bead blasted)	705	200	4.8E-02	3.32
		500	3.0E-07	3.96
		1200	5.0E-07	7.63
	745	200	5.4E-07	11.36
		500	3.5E-07	13.95
		1200	2.5E-07	15.36
	785	200	1.9E-07	15.94
		500	5.6E-07	14.92
		1200	1.2E-07	18.24
S3 (glass powder blasted)	705	200	2.9E-07	4.28
		500	4.4E-07	8.44
		1200	3.7E-07	14.10
	745	200	2.4E-07	18.78
		500	7.3E-07	20.18
		1200	4.9E-07	19.30
	785	200	3.8E-07	18.94
		500	3.9E-07	17.18
		1200	6.2E-07	19.28

Leak rates marked with <sup>a</sup> were measured by pressure gain test only, all other results were measured by helium leak test

### 4 Results and discussion

The results of the leak rate  $Q_L$  and the failure force  $F_F$  for the 27 parameter combinations are presented in Table 2 and Fig. 6. The hermeticity was measured with the pressure gain test for all samples and a second time with helium leak test for samples with values better than  $Q_L < 10^{-4}$  mbar l/s. Ultimately, the adherence was determined for all samples resulting in the destruction of the glass. All results for  $Q_L$  and  $F_F$  are arithmetic mean values calculated from measurements of the 2 samples manufactured with the same parameters. Measurement errors can be estimated by calculating the deviations of the individual measurements from the mean values, resulting in an average error of 20% for  $F_F$  and 40% for  $Q_L$ . While 20% is an acceptable error, 40% for  $Q_L$  appears quite high, but is still relatively small considering the range of results over many orders of magnitude.

The values for the leak rate  $Q_L$  can be divided in two groups. Results of  $Q_L > 10^{-3}$  mbar l/s can be classified as simply not hermetic. The other results around  $10^{-6}$  mbar l/s or better are typical for electronic packaging, medical technology and high vacuum technology according to Kutzke [14]. By applying the separation force  $F_s$  to the glass-to-metal interface area of 117.8 mm<sup>2</sup> a value for the shear pressure required for unbonding can be calculated, resulting in very high values of more than 170 MPa for the best adherence results.

In Fig. 6 the results are illustrated separately for the 3 different surface types. In general, better results with lower leak rates and higher failure forces were achieved with the glass powder blasted metal surface (S3), followed by the glass bead blasted surface (S2) and the milled surface (S1). This corresponds with the results of the roughness

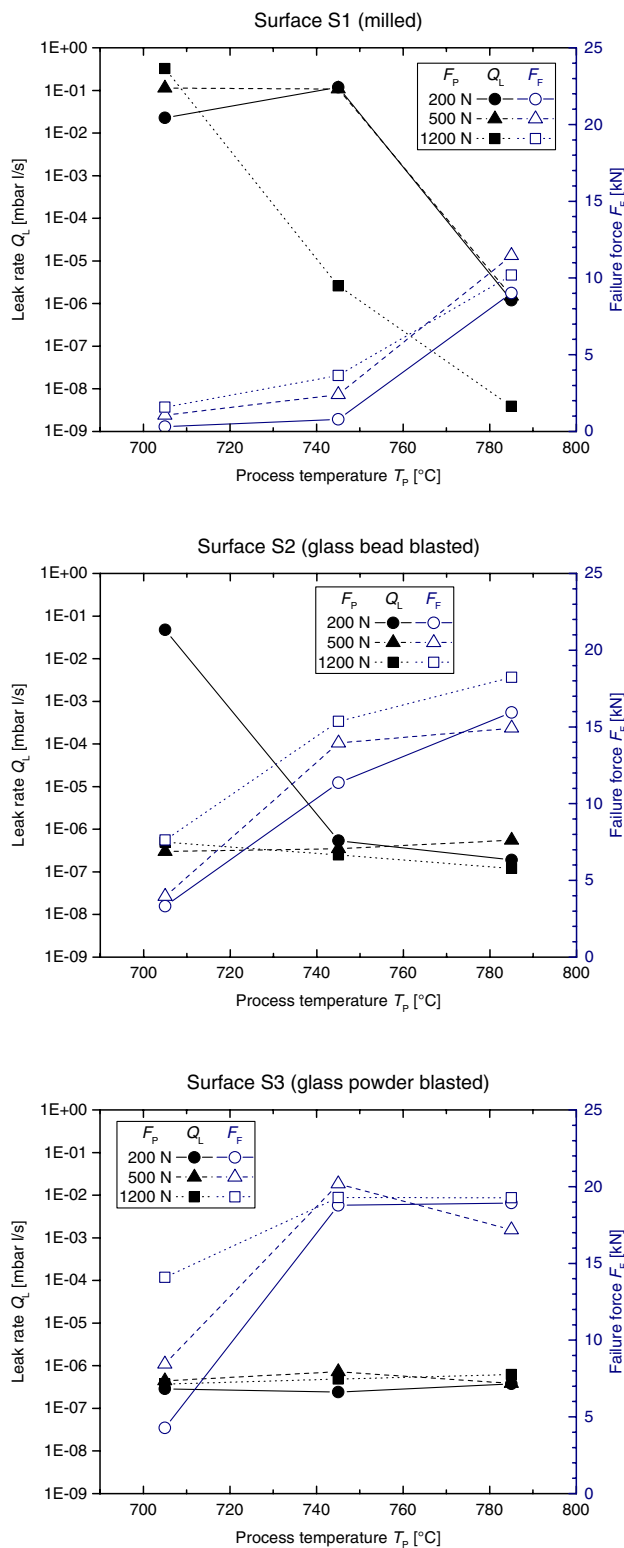


**Fig. 6** Results of leak rate and failure force over process temperature

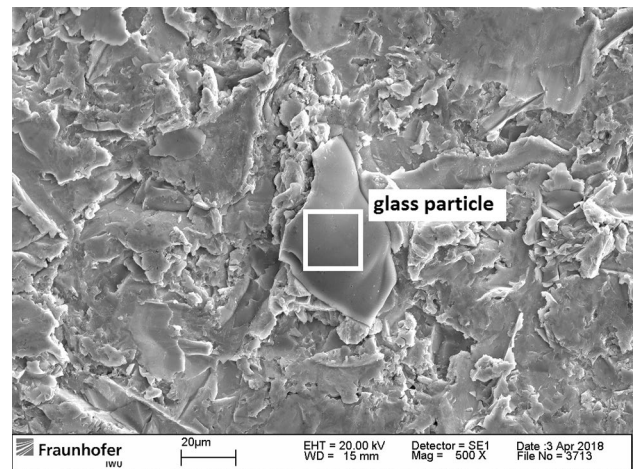


**Fig. 7** SEM image of an S3 surface (glass powder blasted) with a particle sticking in the surface which was identified as glass by EDS analysis (EDS results, glass particle: 60% Si, 40% Na, Ca, K, O/area around glass particle: 80% Ti, 20% Va, Al and other metals)

measurement of  $Ra = 1.71 \mu\text{m}$  (S3),  $Ra = 1.15 \mu\text{m}$  (S2) and  $Ra = 0.34 \mu\text{m}$  (S1). The improvement of adherence by surface roughening can be explained by the effect of mechanical interlocking and may be further improved by residual glass particles mainly found on S3, presumably due to the sharp edges of the glass powder blasting material. Figure 7 shows an SEM image of the titanium surface after glass powder blasting with a glass particle sticking in the surface. The positive influence of surface roughening on the leak rate can be explained by the increased surface area and by a possible surface activation from the blasting effect resulting in improved chemical bonding.

In Fig. 6 for surface S3 it can be observed, that the failure force  $F_F$  increases with higher process temperatures  $T_p$  and also with higher process forces  $F_p$  at the lowest process temperature of  $T_p = 705 \text{ }^\circ\text{C}$ . Because of the higher viscosity at low temperatures it takes high process forces to press the glass into the cavities of the rough surface, while for higher temperatures this is also possible with low process forces because of the reduced viscosity. This effect can be observed for S2 as well, although here it is less pronounced. In both cases it supports the hypotheses that for roughened surfaces the bonding strength is dominated by mechanical interlocking. However, for the relatively smooth surface S1 the failure force also increases with process temperature, although the total values are lower and the process force has less influence on the results. This observation indicates that chemical bonding supported by high process temperatures improves adhesion as a second and comparatively weak effect next to mechanical interlocking.

As described in the introduction, the key to hermetic glass-to-metal bonding is to bring both materials in close

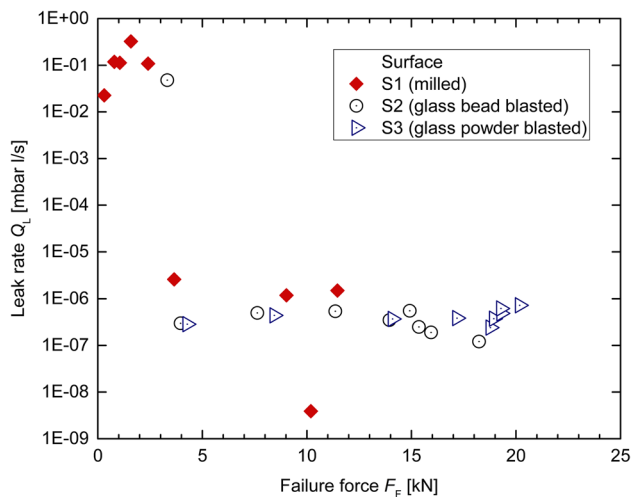


**Fig. 8** Results for leak rate  $Q_L$  versus failure force  $F_F$

contact at atomic scales, which can be achieved by different approaches such as wetting of the metal surface with molten glass or static electric fields in anodic bonding. The results for  $Q_L$  in S3 (Fig. 6) show that for rough metal surfaces this can be achieved at high glass viscosities and low process forces already. This may be explained with the sharp peaks in the rough surfaces which push into the glass material with small cross sections and therefore high local pressure. In contrast to this behaviour, for the smooth surface S1 either high temperatures or increased process forces are required to achieve the necessary close contact between the materials. However, this effect may be mixed with the improvement of favourable chemical reactions at higher process temperatures as described above already.

The very good result of  $Q_L = 3.9 \times 10^{-9}$  mbar l/s (surface S1,  $T_p = 785$  °C,  $F_F = 1200$  N) was confirmed even after the experiment was repeated with 2 additional samples. For this parameter combination ( $T_p$  and  $F_F$ ) roughening of the surface increases adherence while hermeticity is reduced. This may be explained by the increased contact time during the 15 s bonding process. While for smooth surfaces the glass is in full contact with the metal from the beginning, the glass requires some time to be pressed into the pits of a roughened surface.

In Fig. 8 the results of leak rate and failure force are compared directly. Samples with  $F_F < 3$  kN were not hermetic, while for samples of  $F_F > 4$  kN hermeticity is good and does not improve much with higher separation forces.

The results can be analysed for the influence of thermal expansion. When temperatures fall below the set point of the glass during cooling, the stress relaxation of the glass becomes slow and any stress caused by thermal expansion remains in the materials. According to Donald [2] the set point is located near the

glass transition temperature. For B270 this means a temperature between 500 and 550 °C. With the coefficients of thermal expansion (chapter 3.1) and the radius of  $r = 7.5$  mm the contraction of the glass cylinder during cooling from 500 to 20 °C is calculated to  $\Delta r = 37$   $\mu\text{m}$ , while the inside radius of the titanium ring only decreases with  $\Delta r = 34$   $\mu\text{m}$ . Since the glass contracts slightly more than the metal, the sealing cannot be classified as a compression seal but as a matched seal or (slightly) unmatched seal. The residual tensile stress at the glass-titanium interface may be a reason for failure at the interface and poor results for bonding strength and hermeticity.

## 5 Summary and conclusions

A new glass-to-metal bonding method was successfully applied for production of hermetic and mechanically strong seals between glass and titanium. The influence of the 3 process parameters metal surface, process temperature and process force on the leak rate and the bonding strength was investigated experimentally. The following conclusions can be drawn from the results of these investigations.

A higher surface roughness generally improves hermeticity and bonding strength. Increasing  $R_a$  by a factor of 5 leads to an average increase of failure force by a factor of 3. Furthermore, the percentage of hermetic sealings increases from 50 to 100%.

Raising the process temperature from 705 to 785 °C significantly improves the bonding strength (failure force three times higher) and the leak rate. On the other hand, a higher process force has relatively small influence on bonding strength and hermeticity. Raising the process force from 200 to 1200 N only increases the failure force by approx. 10% on average.

The experimental results can be explained by the effects of mechanical interlocking, direct bonding based on close contact and chemical bonding between the 2 materials. For the verification of the hypotheses derived from the experiments further investigations of the interfaces after bonding, e.g. by SEM and EDS are recommended.

**Acknowledgements** The work was developed as part of the Fraunhofer pilot project Theranostic Implants—Approval-relevant development of key technologies for medicine. We would like to gratefully thank the Fraunhofer-Gesellschaft for its support.

## Compliance with ethical standards

**Conflict of interest** The authors declare that they have no conflict of interest.

## References

1. Briand D, Weber P, De Rooij NF (2004) Bonding properties of metals anodically bonded to glass. *Sens Actuators A Phys* 114:543–549
2. Donald I (1993) Preparation, properties and chemistry of glass-and glass-ceramic-to-metal seals and coatings. *J Mater Sci* 28:2841–2886
3. Donald I (2009) Glas-to-metal seals. Society of Glass Technology
4. Donald I, Mallinson P, Metcalfe B, Gerrard L, Fernie J (2011) Recent developments in the preparation, characterization and applications of glass-and glass-ceramic-to-metal seals and coatings. *J Mater Sci* 46:1975–2000
5. Fraunhofer-Gesellschaft zur Förderung der angewandten Forschung e.V. (2017) Housing component, and method for manufacturing same. 2017-05-11. WO 2017/194685 A1
6. Goldstein JI, Choi SK, Loo FJ, Bastin GF, Metselaar R (1995) Solid-state reactions and phase relations in the Ti–Si–O system at 1373 K. *J Am Ceram Soc* 78:313–322
7. Goller G (2004) The effect of bond coat on mechanical properties of plasma sprayed bioglass-titanium coatings. *Ceram Int* 30:351–355
8. Gomez-Vega J, Hozumi A, Saiz E, Tomsia A, Sugimura H, Takai O (2001) Bioactive glass–mesoporous silica coatings on Ti6Al4V through enameling and triblock-copolymer-templated sol–gel processing. *J Biomed Mater Res Part A* 56:382–389
9. Gomez-Vega J, Saiz E, Tomsia A (1999) Glass-based coatings for titanium implant alloys. *J Biomed Mater Res* 46:549–559
10. Khandan O, Stark D, Chang A, Rao MP (2014) Wafer-scale titanium anodic bonding for microfluidic applications. *Sens Actuators B Chem* 205:244–248
11. King BW, Tripp H, Duckworth WH (1959) Nature of adherence of porcelain enamels to metals. *J Am Ceram Soc* 42:504–525
12. Kitsugi T, Nakamura T, Oka M, Senaha Y, Goto T, Shibuya T (1996) Bone-bonding behavior of plasma-sprayed coatings of BioglassR, AW–glass ceramic, and tricalcium phosphate on titanium alloy. *J Biomed Mater Res* 30:261–269
13. Kuckert H, Born C, Wagner G, Eifler D (2001) Helium-tight sealing of glass with metal by ultrasonic welding. *Adv Eng Mater* 3:903–905
14. Kutzke K (1998) Dichtheitsprüfungen und Lecksuche mit dem Helium-Leckdetektor: ein Leitfaden zum praktischen Einsatz bei der Qualitätssicherung und Wartung. expert verlag
15. Lei D, Wang Z, Li J, Li J, Wang Z (2012) Experimental study of glass to metal seals for parabolic trough receivers. *Renew Energy* 48:85–91
16. Li T, Zhang Y, Luo J, Chen J (2014) Field-assisted titanium-glass bonding. In: 2014 9th IEEE international conference on nano/micro engineered and molecular systems (NEMS), pp 362–365
17. Lopez-Esteban S, Saiz E, Fujino S, Oku T, Suganuma K, Tomsia AP (2003) Bioactive glass coatings for orthopedic metallic implants. *J Eur Ceram Soc* 23:2921–2930
18. Luetjering G, Williams JC (2007) Titanium. Springer, Berlin
19. Passerone AP, Valbusa G, Biagini E (1977) The titanium–molten glass system: interactions and wetting. *J Mater Sci* 12:2465–2474
20. Pazo A, Saiz E, Tomsia A (1998) Silicate glass coatings on Ti-based implants. *Acta Mater* 46:2551–2558
21. Peddi L, Brow RK, Brown RF (2008) Bioactive borate glass coatings for titanium alloys. *J Mater Sci Mater Med* 19:3145–3152
22. Wei J, Xie H, Nai M, Wong C, Lee L (2003) Low temperature wafer anodic bonding. *J Micromech Microeng* 13:217
23. Winkler S, Edelmann J, Welsch C, Ruff R (2017) Different encapsulation strategies for implanted electronics. *Curr Dir Biomed Eng* 3(2):725–728

**Publisher's Note** Springer Nature remains neutral with regard to jurisdictional claims in published maps and institutional affiliations.